Available online at www.sciencedirect.com

ScienceDirect

Energy Procedia

Energy Procedia 92 (2016) 939 – 948

6th International Conference on Silicon Photovoltaics, SiliconPV 2016

Double printing nPERT cells with narrow contact layers

Jan Lossen[a]*, Dominik Rudolph[a], Lejo J. Koduvelikulathu[a], Ricardo Carvalho[b], Mark P. Rossetto[b], Oscar Borsato[c], Emiliano Bortoletto[c], Marco Galiazzo[c]

[a]*ISC Konstanz e. V., Rudolf-Diesel-Straße 15, 78467 Konstanz,Germany*
[b]*MegaCell srl, Via Postumia 9/B, 35010 Carmignano di Brenta (PD), Italy*
[c]*Applied Materials Italia, Via Postumia Ovest 244, 31048 Treviso, Italy*

Abstract

Screen printing of two different paste layers on top of each other is used for reducing the detrimental effect of the p+ contact to nPERT cells. For the contacting layer, a line width between 15 µm and 30 µm is used. In a second print step, using a wider opening, these contacting layers are augmented by a non-contacting paste layer to form a line of sufficient conductivity. Reduced shading and a smaller contact area lead to increased J_{SC} and V_{OC}. Still, an excessive reduction of the contact area causes an increase of contact resistivity compensating the gain. For an optimum configuration, an efficiency gain of up to 0.2%$_{abs}$ and a reduction of paste consumption by 10 mg are demonstrated on precursors from industrial production.

Peer review by the scientific conference committee of SiliconPV 2016 under responsibility of PSE AG.

Keywords: screen printing; nPERT; contact formation; n-type; double printing

1. Introduction

The nPERT cell (a passivated emitter rear totally diffused solar cell on n-type wafer) offers several advantages compared to p-type cells of similar complexity, such as PERC cells: the lack of boron-oxygen degradation in the bulk, high transparency of boron emitters and easily obtained high bifacial ratio between front and rear side. However, one of the main disadvantages of screen printed cells from this type is that silver pastes containing aluminum particles, allowing for a low contact resistance to the p+ emitter, typically lead to strong recombination

* Corresponding author. Tel.: +49-7531-36183360; fax: +49-7531-3618311.
E-mail address: jan.lossen@isc-konstanz.de

Peer review by the scientific conference committee of SiliconPV 2016 under responsibility of PSE AG.
doi:10.1016/j.egypro.2016.07.105

beneath the contacts, evident by a huge drop from the implied Voc value of a precursor to the Voc of the ready cell [1]. The corresponding J_{0met} value had been determined to be as high as 4300 fA/cm^2 [2]. In an actual study with improved contact paste and optimized emitter profiles J_{0met} still amounts 2500 fA/cm^2 [3].

Extensive research has been dedicated to describe the contact formation [4] and model the origin of the loss [5, 6]. Recently it has been shown that Al-free contacts to boron emitters are possible [7, 8], but it has not been demonstrated yet that this allows for the fabrication of solar cells with superior properties.

Having said that, double printing has in the last years shown to be a viable option for industrial production, paying off increased requirements on printers and screens by a better aspect ratio, resulting in reduced shading, and by reduced silver consumption [9]. As most metallization lines are equipped with three printers, nPERT cells are often metalized with dual print on the front side, with bus bars being printed separately from the fingers. By using a non-contacting paste for the bus bars, V_{OC} is increased by more than 3 mV in comparison to single print [10]. So the additional effort for double printing is minimal. Basically it consists in undertaking measures to assure good alignment of the two prints.

As on the one hand contact resistance of Al-Ag-paste to the boron emitter can be quite low, recently values below 1 mOhm/cm^2 have been reported [6], and on the other hand the J_{0_metal} is significant, we explore in this work the use of extremely narrow contact layers in order to mitigate the detrimental effect of the contact by reducing its area. Therefore, unlike in other double printing work, the first layer L1 of contacting Ag-Al-paste, is printed with a narrower screen opening than the second layer L2 of non-contacting conduction paste. See Fig. 1 (c) for the concept.

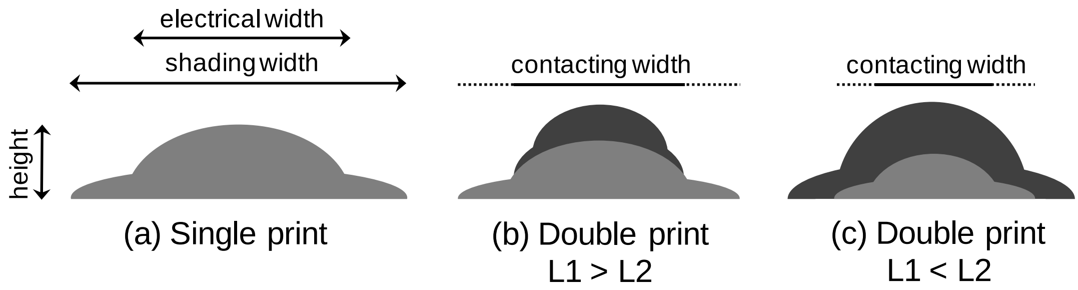

Fig. 1 (a) Schematic drawing of the cross section of a single printed finger. Typically only a core section has significant height. We define its width as electrical width of the finger. The total width covered by metal, as e.g. determined in a SEM picture, we define as shading width. (b) Schematic cross section of a double printed finger, with layer L1 broader than layer L2. It seems reasonable to suspect that the width on with a contact to the emitter is formed is some value between shading width and electrical width of L1. (c) In the case of double printing with layer L1 narrower than layer L2, the contacting width is reduced more drastically.

2. Experimental

We performed a series of print experiments on BiSoN solar cell precursors from the industrial production of MegaCell srl. BiSoN is a bifacial nPERT cell featuring diffused boron front side emitter and phosphorous BSF and a low cost passivation based on an interfacial BSG layer. Further details on the cell structure and the process technology can be found previous work [11, 12]. Within each experiment the wafer quality and pre-process are kept constant, but as the experiments are performed over duration of several months, some variations in wafer material and pre-processing over the complete set of experiments cannot be excluded.

Screen printing is performed at the print labs of ISC in Konstanz, Germany and of Applied Materials in Treviso, Italy, using print-on-print alignment for the double prints. We use commercial silver and silver-aluminum pastes, and high precision MICRON^{TM} screens from the company PVF.

IV measurements are performed on a flasher calibrated to an appropriated reference cell certified by Fraunhofer ISE CalLab under black chuck conditions. Contact resistivity is measured according to the transfer-length-method (TLM) by 4-point probing on 10 mm wide samples with equidistant metallization lines, using a GP Tester.

3. Results

3.1. Simulations

In order to understand the influence of contact width on the electrical parameters of nPERT solar cells, a series of parameter variations is performed using the software package Griddler 2.5 Pro from SERIS [13].

The reference model is set up using measured input parameters for line resistances, sheet resistances and saturation current densities of a BiSoN cell with η ~ 20%. The front metal grid layout is composed of three 1.45 mm wide bus bars and 60 µm wide fingers with line resistance of 0.45 Ω/cm and J_{0met} of 2500 fA/cm^2. To model only the influence of contact width of a double printed stack, we reduced the contact width for a set of contact resistivities while maintaining line resistance. The capability of double printing to deposit fingers of higher aspect ratio allowing for reduced optical shading, is excluded deliberately from the simulation, by assuming identical optical shading, e.g. constant short circuit current Jsc.

Fig. 2 summarizes the simulated effects on FF and Voc and the resulting effect on efficiency. With shrinking contact widths, we observe a gain in Voc arising due to the reduced area affected from metal recombination. However, the FF of the cell decreases due to an increased contribution of contact resistance to the series resistance of the cell.

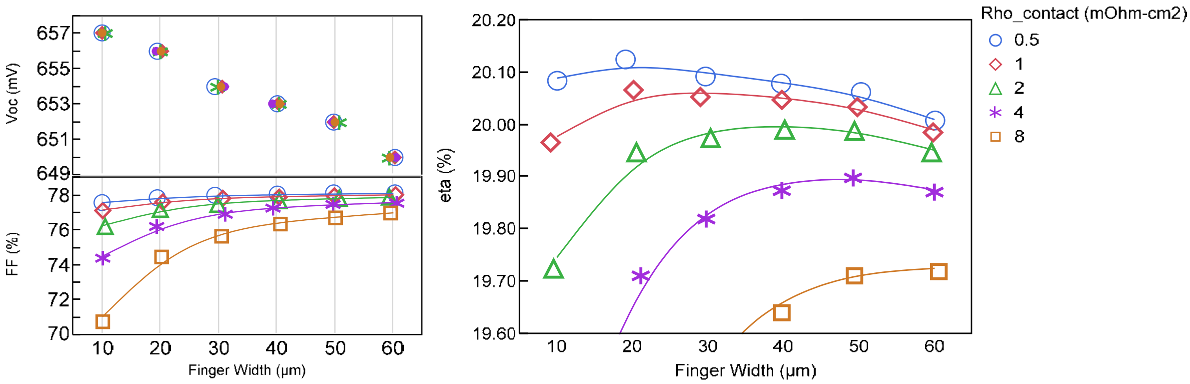

Fig. 2: Simulated electrical parameter for varying contact width and specific resistivity.

As the effects of increasing Voc and decreasing FF compete, the resulting effect on the efficiency is smaller. For high contact resistivity of 8 mΩcm^2, the optimum contact width is 60 µm or above. With lower contact resistivity the optimum contact width shifts to lower width. For a contact resistivity of 1-2 mΩcm^2 a contact width of 30-40 µm is optimum, allowing for a 3-4 mV increased V_{OC}, without reducing FF significantly.

3.2. Double printing with very narrow line width

In a first double printing experiment a finger grid (L1) was printed with Ag-Al contacting paste from a screen with only 20 µm wide openings. An in a second step (L2) wider fingers and bus bars are printed on top with three different pastes, as described in Table I. One of the groups was printed a third time to see the effect of a higher paste lay-down. As a reference, dual printing with 38 µm wide line openings and the same line count was used.

Table I – screen parameter, paste type of second print and lay-down for the groups of the first experiment

Print		Ref	DP_A	DP_B	DP_C	TP_B
L1	line opening width [µm]	38	20	20	20	20
	paste lay-down [mg]	67	31	31	31	31
L2	line opening width [µm]	(Only BB)	38	38	38	38
	paste type and lay-down (lines + BB) [mg]	A / 60	A / 75	B / 71	C / 93	B / 71+65

As shown in Fig. 3, the double and triple printed groups have increased J_{SC} due to the reduced shading of the lines. For most groups V_{OC} is also increased as expected, due to the reduced contact area. However, one of the pastes used for the second print, paste type C, results in a reduced Voc and FF. It obviously creates additional damage in the overlapping line area and beneath the BB and is not suitable as non-contacting paste. The other L2 pastes perform quite similar. The additional layer of paste B in the triple print group has almost no effect. Neither does it cause additional shading, nor does it increase the FF much further. The gain in efficiency compared to the reference group is almost 0.3%, but the reference group lacks in FF probably caused by increased line resistance on account of too low paste lay-down and stays behind the efficiency potential know from prior experiments.

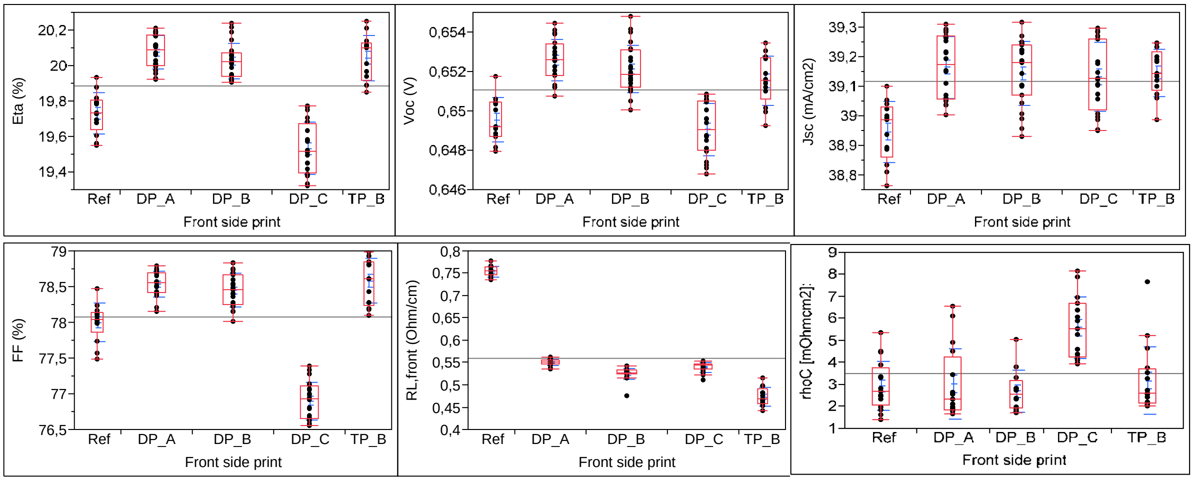

Fig. 3: IV parameters and resistance measurements of double printed cells with different L2 layers

In order to investigate the influence of the L1 print more systematically we combined in a second experiment L1 prints with opening widths of 15, 20 and 25 µm with L2 prints from screens with different width and EOM height. Fig. 4 shows the applied combinations and the achieved paste lay-downs. With higher paste lay-down during L1 the paste transfer during L2 print decreases, as the cavity in the screen is partly filled up by the layer already present at the substrate. The line width of the complete double printed finger stack, determined by laser scanning microscope measurement on four positions per wafer, increases with total paste lay-down with some differences for the screen combinations, probably due to slight differences in matching of the screens. The shading width, as defined in Fig. 1, of the double printed fingers is in the range of 50 to 60 µm and hence only slightly reduced against the 65 µm wide reference finger.

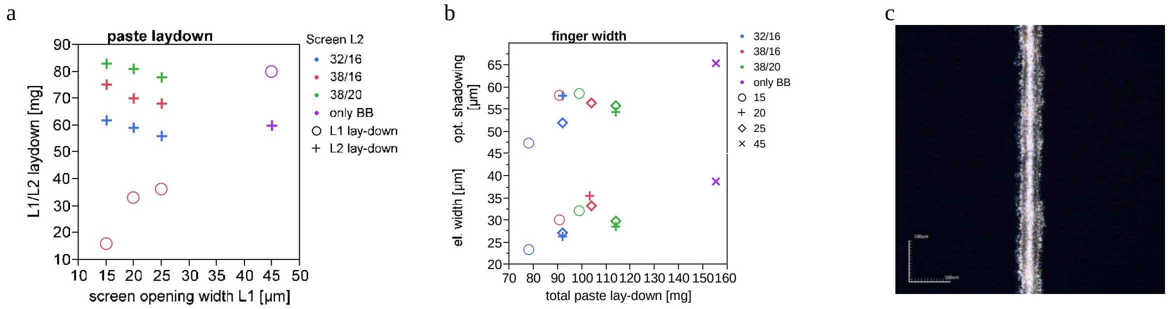

Fig. 4 (a) Paste lay-down for double printing with different screen combinations (b) finger width after fast firing as function of paste lay-down (c) laser scanning microscopy picture of fired finger with L1 opening 25 µm and L2 screen of 38 µm opening and 20 µm EOM.

From these, six groups with higher L2 paste transfer have been selected for a test on solar cells. A dual printed reference group with typical paste lay-down *(0_Ref)* and additionally a dual printed group with increase paste lay-down *(1_DuP_H)* are included, see Table II.

Table II –Test matrix of second double printing experiment

Print		0_Ref	1_DuP_H	2_DP15L	3_DP20L	4_DP25L	5_DP15H	6_DP20H	7_DP25H
L1	line opening width [µm]	45	45	15	20	25	15	20	25
L2	line width [µm] / EOM [µm]	only BB	only BB	38/16	38/16	38/16	38/20	38/20	38/20
both	Total paste lay-down fs [mg]	140	155	91	103	104	99	114	114

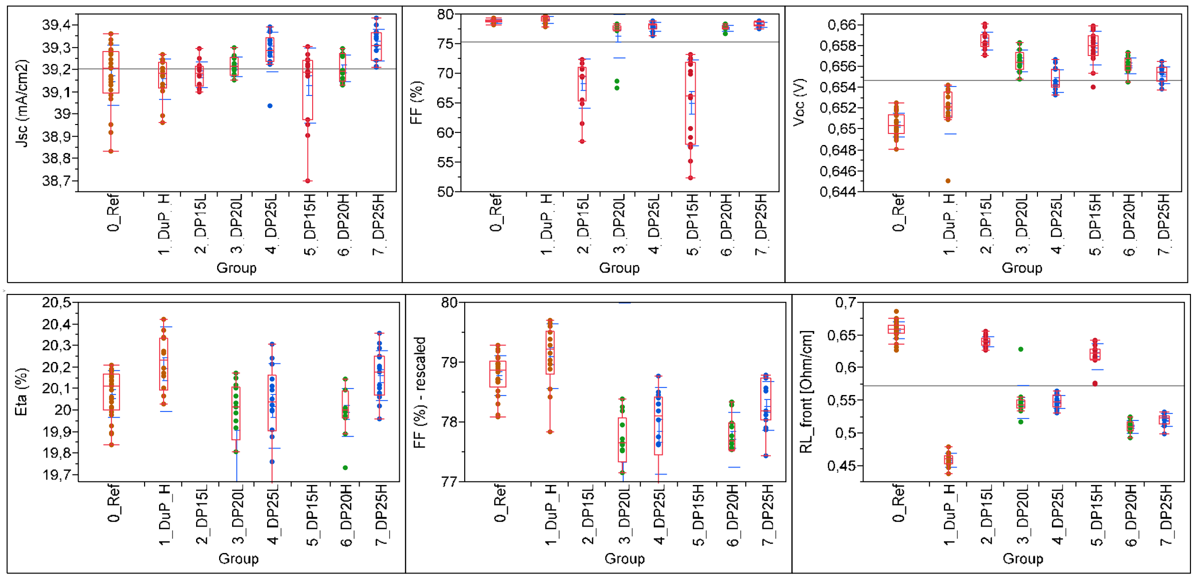

Fig. 5 Electrical parameters of double printed *(DP)* solar cells with varying L1 width and L2 lay-down, compared with dual printed cell of different paste lay-down. Details on the screen parameters are given in Table II. Compared with the reference, both the dual print with high paste lay-down *(DuP_H)* and double print with L1 width of 25 µm *(DP25H)* yield increased efficiency.

IV parameters of the cells are given in Fig. 5. The groups printed with the narrowest L1 openings of 15µm exhibit a strongly reduced FF around 65%, limiting the efficiency to values around 17%, not displayed in this scaling. For the other groups median efficiencies are similar in the range of 20.1% ± 0.1%. As expected from the simulation a smaller L1 width leads to clearly increased Voc, but reduced FF. However, not only the *DP15* groups, but also the groups with broader L1 layers have lower FF than expected from simulation. TLM measurements reveal, as show in Fig. 6, that the additional decrease of FF arises from an increased specific contact resistance. Electroluminescence pictures confirm this finding, showing inhomogeneous luminescence, typical for increased contact resistance.

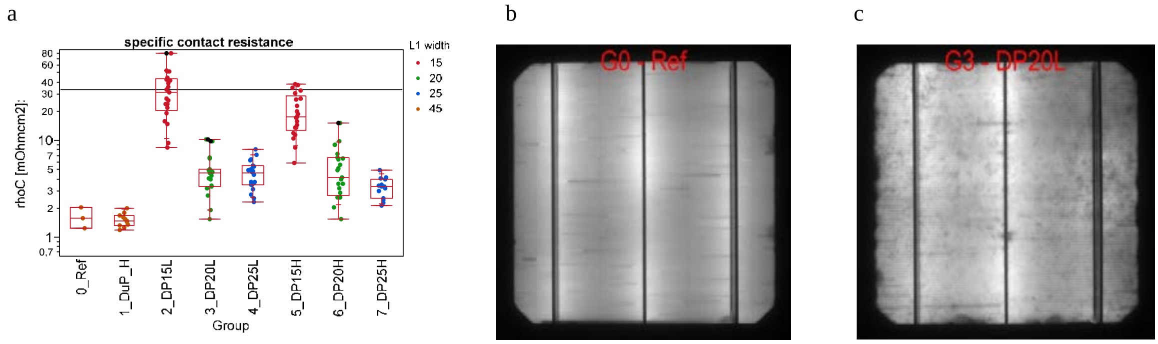

Fig. 6 (a) Contact resistivity of samples from the second print experiment (b/c) electroluminescence pictures on two cells

3.3. Influences on contact resistivity

Several mechanisms could be responsible for the rise in contact resistivity: Either, the glass frit from the contacting paste mixes with the glass frit of the non-contacting paste during firing, resulting in a deteriorated contacting behavior. Or, the absolute volume of contacting paste simply becomes too low in order to contain sufficient glass frit, aluminum particles or other components per area of the contact, e.g. the height of L1 is too low. Besides, increased storage between L1 print and fast-firing could have a detrimental influence as, due to practical reasons, we typically conduct L1 and L2 prints on different days.

In order to test these hypotheses, an experiment on TLM samples is conducted. Three groups of L1 prints are created: very narrow lines from a 20 µm opening are printed on two different days with four days storage time in between and wider lines from a 38 µm opening are printed on the second printing day. Each of the L1 groups is

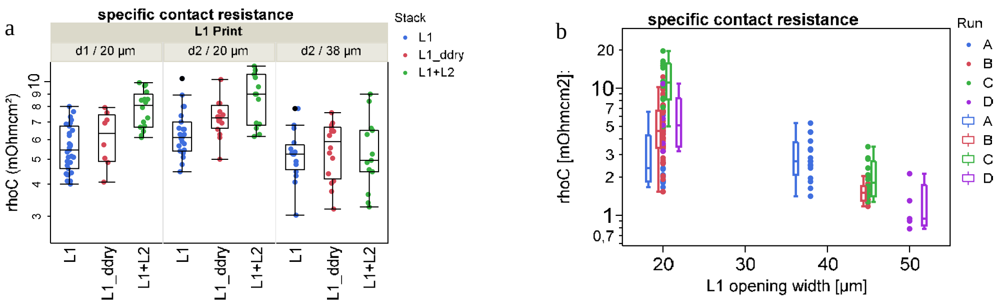

Fig. 7 (a) Contact resistivity of L1 layers of different width and print date, submitted to no further treatment (blue symbols), additional excessive drying (red symbols) or capping with L2 paste (green symbols). (b) Contact resistivity of double printed and single printed fingers from different experiments plotted in one graph.

submitted to three different post treatments and fast firing, all conduced promptly after L1 prints on the second day: (a) no treatment *(L1)*, (b) additional excessive drying at 200°C for 20 minutes *(L1_ddry)*, (c) capping by additional L2 print of non-contacting paste and drying *(L1+L2)*. After fast firing of all samples, the contact resistivity is determined by TLM measurements on three wafers per group, as displayed in Fig 7 (a). For the very narrow contact layers from the 20 µm opening, both excessive drying and capping with non-contacting paste seem to have a certain detrimental influence on the contact resistivity, while we rate the effect of four days storage after L1 print (d1 vs. d2) to be negligible. However, for the wide contact layers from the 38 µm opening, contact resistivity is generally lower, and the different post treatments have no or little influence.

For further insight, in Fig. 7 (b), the contact resistivities of single and double printed groups of different experiments are plotted in one graph. For the double printed stacks, which are the four groups with opening width of 20 µm, huge variations in the contact resistivity can be observed in the different experiments. The single printed reference groups exhibit in general lower and more uniform values, with the trend that increased width results in lower contact resistivity. We rate this to be the dominant effect, arising probably from the reduced height of the paste layer, when printed from a screen with narrower opening.

In order to mitigate this problem, in a third solar cell experiment the height of the L1 layer is increased artificially by printing contacting paste twice from the same screen, before depositing a L2 layer of non-contacting paste *(TP20)*. This, as shown in Fig. 8 (a), indeed helps to decrease the contact resistivity, though on the measured sample the absolute values are still quite high. Fig. 8 (b) shows the FF of the different groups. The median FF of the triple printed group is increased and at least some of the cells feature FF above 78.5% without compromising the V_{OC} gain attributed to the smaller contact width. Table III summarizes the cell results. Two champion cells have efficiencies of 20.49 %.

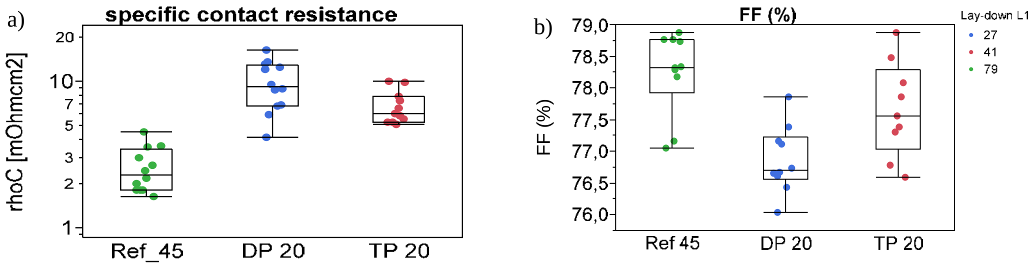

Fig. 8 Contact resistivity (measured on one cell per group) and FF of cells from the third solar cell experiment, comparing a single printed reference group (Ref 45) with a double printed group with 20 µm L1 width and a triple printed group (2x L1 from 20 µm opening, 1 x L2 from 38 µm opening).

Table III: IV parameters of the reference group and the triple print group.

Group		number of cells	Voc (V)	Jsc (mA/cm^2)	FF (%)	Eta (%)
Ref 45	median	10	0.653	39.48	78.32	20.16
	best	1	0.654	39.54	78.88	20.36
TP 20	median	9	0.657	39.65	77.56	20.22
	best	1	0.658	39.77	78.87	20.49

3.4. Double printing with moderate line width

As the foregoing experiments showed that with current Ag-Al paste it is difficult to achieve reliably low contact resistance with very narrow contact layers, in a final experiment the benefits of double printing with moderate contacting width of 30 µm is assessed. Experimental details and resulting geometries are summarized in Table IVIV.

Table IV: Experimental matrix, lay-down and geometrical data of the experiment on double printing with moderate line width

lot	group	process	opening width	m L1 (mg)	m L2 (mg)	m L3 (mg)	total lay-down (mg)	height (µm)	width (µm)	A/R
1	DuP	Ref	45	80	55		135	15.5	55.3	0.28
2	DP1	2x L1 paste	30 + 38	41	91		132	17.9	45.1	0.40
3	DP2	L1 paste + L2 paste	30 + 38	41	83		124	17.1	48.3	0.35
4	TP	2x L1 p. + L2 paste	30 + 38	41	26	72	139	16.2	44.1	0.37

All double printed groups feature reduced line width and increased aspect ratio. Assuming a reduction of shaded width by 10µm per finger, an increase of short circuit current of around 0.6% could be expected, which is in the lower end of range of the I_{SC} gains actually observed on the cells, compare Fig. 9. V_{OC} is also slightly increased for all groups besides DP1, which does not feature floating busbars. FF on the other hand is for the double printed groups using the two different pastes (*3_DP2* and *4_TP*) still slightly decreased, with little difference between double and triple printing. Altogether, the double printed group DP2 yields an increase of efficiency of $1\%_{rel}$ or $0.2\%_{abs}$ while reducing the total lay-down by around 10 mg.

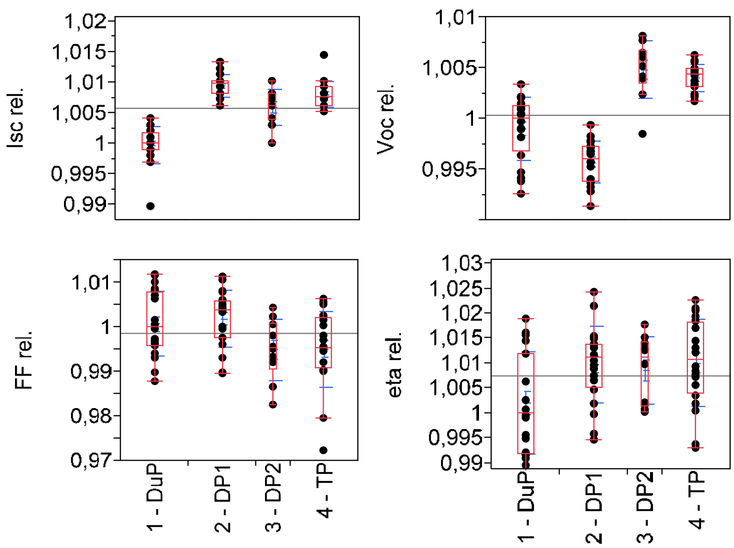

Fig. 9: Relative IV data of 4BB cells with dual and double printing, according to Table IV

4. Discussion and conclusions

In summary of the experiments with very narrow L1 layers it can be stated that screen printing through openings of around 20 µm is possible and leads, as expected from the reduced contact area, to solar cells with increased V_{OC}. Nevertheless, contact resistivity of the narrower contacts is increased and features a higher variability, which results, to a more pronounced decrease of FF than expected from the reduced contact area, leveling the gain in V_{OC}. An explanation could be, that the composition of the paste is optimized for these very fine lines, but rather for lines > 50 µm. Possibly an adjusted composition could overcome the problem.

It should be remarked, that we did not perform any micro-analysis of the contacts in this study. Neither the area showing microscopic signs of contact formation was determined, nor data as crystallite density or crystallite depth distribution. All contact resistivities were calculated from the shading width of the L1 layer, e.g. the area covered by contacting paste. Any apparent increase in contact resistivity therefore could also be explained as a reduction of the true contact area at constant or even improved contact resistivity. For example could the effect of a L2 capping on the contact resistance of the 20 µm L1 layer, compare Fig. 7 (a), be suspected to origin from glass of the L2 layer creeping under the L1 layer reducing its true contacting width. But then, in the case of the L1 layer from the 15 µm wide opening, measured with LSM to have a shading width of 34 µm, the assumption of a constant contact resistivity would request a true contact width of less than 5 µm, which is unlikely to be build uniformly. On microscopic scaled it is anyway useless to speak of uniform contact resistivity, as crystallites in the size of micros are assumed to promote the electrical contact.

We suspect that both effects might play a role: a reduction of the area fraction of contacted regions versus metal covered area, and the area density of low resistive contact points within this fraction. As we cannot dissolve these effects with our methodology, we prefer to describe the macroscopic effect as a reduction of specific contact resistance in relation to the area covered with contacting paste.

However, it is worth to notice that the champion cells of the double and triple printed groups have similar FF, but consistently higher V_{OC} as champion cells from reference groups. E.g. contact resistance of these cells is sufficiently low, while recombination arising from the contacts is reduced. Nevertheless as the spread within the groups and from run to run increases the very narrow contact layers are currently not suitable for industrial production. The picture might change with pastes optimized for such small line width.

Nonetheless, double printing with moderate line width still leads to a similar increase of Jsc due to smaller line width and increased aspect ratio. The Voc gain by reduced contact area is diminished, but so is the risk for an increase in series resistance. For a combination of a 30 µm wide L1 and 38 µm wide L2 layer, on average an efficiency gain of 0.2% could be demonstrated while total paste lay-down was reduced by 10 mg.

Acknowledgements

The authors would like to thank the company PVF-Vertriebs GmbH for supplying high accuracy MICRON™ screen for the experiments and coping with layout changes on short notice.

Further we would like to thank technicians and operators at ISC in Konstanz, Applied Materials in Treviso and MegaCell in Carmignano for their support and their patience.

References

[1] A. Edler, V.D. Mihailetchi, C. Comparotto, L.J. Koduvelikulathu, R. Kopecek, R. Harney, T. Böscke, J. Lossen, On the Metallization Losses of Bifacial n-Type Silicon Solar Cells, 27th European Photovoltaic Solar Energy Conference and Exhibition, Frankfurt, 2012

[2] Alexander Edler, Valentin D. Mihailetchi, Lejo J. Koduvelikulathu, Corrado Comparotto, Radovan Kopecek and Rudolf Harney, Metallization-induced recombination losses of bifacial silicon solar cells, Prog. Photovolt: Res. Appl. 2015; 23:620–627

[3] V. D. Mihailetchi, H. Chun, G. Galbiati, R. Kopecek, Mitigating Metallization Losses on Boron Emitters of Screen Printed n-type Solar Cells, 6th International Conference on Crystalline Silicon Photovoltaics Silicon PV, Chambery, 2016

[4] S. Fritz, S. Riegel, A. Herguth, M. König, M. Hörteis, G. Hahn, Preservation of Si surface structure by Ag/Al contact spots – an explanatory model Energy Procedia 67 (2015) 43 – 48

[5] N. Wöhrle, et al., Development, Characterization and Modelling of Doping Profile, Contact Resistance, and Metal Spiking in Diffused and Screen-Printed Boron Emitters, Proceedings of the 31st European Photovoltaic Solar Energy Conference and Exhibition, Hamburg, Germany, 2015

[6] Elmar Lohmüller, Sabrina Werner, Rene Hoenig, Johannes Greulich, Florian Clement, Impact of boron doping profiles on the specific contact resistance of screen printed Ag–Al contacts on silicon, Solar Energy Materials and Solar Cells, Volume 142, November 2015, Pages 2–11, Proceedings of the 5th International Conference on Crystalline Silicon Photovoltaics SiliconPV, 2015

[7] J. Engelhardt, A. Frey, S. Fritz, G. Micard, S. Riegel, G. Hahn, B. Terheiden, Contact Formation on Boron Doped Silicon Substrates from Passivating PECV-Deposited Dielectric Doping Layers with Anti-Reflective Properties by Screen-Printing Ag Pastes for High-Efficiency N-Type Silicon Solar Cell , Proceedings of the 31st European Photovoltaic Solar Energy Conference and Exhibition, Hamburg, Germany, 2015

[8] S. Fritz, E. Emre, J. Engelhardt, S. Ebert, N. Nowak, Contacting BBr3-based Boron Emitters with Al-free Screen-printing Paste, 6th International Conference on Crystalline Silicon Photovoltaics Silicon PV, Chambery, 2016

[9] M. Galiazzo, et al., Extensive Comparison of Solar Modules Manufactured with Single and Double Printed Cells, Energy Procedia 77 (2015) 520 – 526

[10] A. Voltan, M. Galiazzo, F. Oberholtzer, M. Emsley, C. E. Dubé and J. Graff, Cell efficiency improvement of fully implanted nPERT solar cells realized through metallization optimization, Proceedings of the 31st European Photovoltaic Solar Energy Conference and Exhibition, Hamburg, Germany, 2015

[11] V.D. Mihailetchi, J. Jourdan, A. Edler, R. Kopecek, R. Harney, D. Stichtenoth, J. Lossen, T. Böscke, H.-J. Krokoszinski, Screen Printed n-Type Silicon Solar Cells for Industrial Application, Proceedings of the 25th European Photovoltaic Solar Energy Conference and Exhibition / 5th World Conference on Photovoltaic Energy Conversion, Valencia, Spain, 2010

[12] Jan Lossen, Florian Buchholz, Corrado Comparotto, Stephan Eisert, Joris Libal, Valentin D. Mihailetchi, Eckard Wefringhaus, Mark Rossetto, Diego Discato, Franco Traverso, From Lab to Fab: Bifacial n-Type Cells Entering Industrial Production, Proceedings of the 31st European Photovoltaic Solar Energy Conference and Exhibition, Hamburg, Germany, 2015

[13] J. Wong, Griddler: Intelligent computer aided design of complex solar cell metallization patterns, Proc. 39th IEEE Photovoltaic Specialists Conference, Tampa, 2013 & J. Wong & R. Sridharan, Griddler 2.5 Pro, http://www.seris.sg/Seris/OurServices/Griddler.html